Research on Energy-saving Renovation and Energy Consumption Correlation of Historical Residential Districts under the Background of Urban Renewal: A Case Study of Hehua Tang District in Nanjing City

Lin Lin, Jin Xing
Affiliation: School of Architecture, Southeast University, Nanjing, Jiangsu Province, China
Email:17816377669@163.com ; jxining@163.com

Abstract
Amid rising global energy demands and China's shift toward urban stock optimisation, this study investigates low-carbon renewal strategies for Nanjing's Lotus Pond Historical District using parametric modelling and energy simulations. Integrating Rhino/Grasshopper with a simulated annealing algorithm, multiple building height schemes were generated and evaluated for solar potential. Results demonstrated optimised schemes reduced energy use intensity (EUI) by 5.6–25 kWh/m² versus baseline. Shape coefficient strongly correlated with EUI (r=0.997), while floor area ratio (FAR) showed inverse correlation (r=-0.989). Vertical building distribution critically influenced solar gains, with self-shading reducing potential by 22%–28% in select cases. Balancing heritage preservation with energy performance, recommendations advocate limiting heights (1–2 stories), optimising shape coefficients (≤0.55), and integrating solar systems. The methodology offers data-driven insights for sustainable historical district renewal in stock-optimisation contexts.

Key words: Energy-efficient Retrofitting Historic Residential District Building Morphology Building Energy Use Intensity

Introduction

According to data from the International Energy Agency (IEA, 2022), global energy consumption increases at a rate of 6% every five years. In China, building energy consumption accounts for 28% to 30% of total societal energy use, with residential buildings contributing 61.7% of this figure[1]. The energy efficiency and emission reduction challenges in China's building sector remain a persistent focus.

Existing studies demonstrate a strong correlation between urban morphology and building energy consumption. Mutual shading between buildings influences the distribution and reflection of solar radiation, thereby affecting energy demands for lighting, cooling, and heating[2]. For instance, Mengju et al. investigated urban morphological parameters of dormitory blocks at Wuhan University, revealing that block topology and urban morphology significantly impact energy consumption and solar potential at the neighbourhood scale[3]. Similarly, Shen et al. evaluated urban morphological factors affecting photovoltaic potential and energy consumption in residential areas in Wuhan, proposing sustainable planning strategies for central China through regression analysis[4]. Researchers have introduced quantitative metrics, such as coverage ratio, average building height, and floor area ratio (FAR), to directly assess relationships between urban form and energy use. Y. Li et al. found that increasing FAR reduces heating energy density, particularly in its initial stages[5], while H. Leng et al. identified FAR as the most critical factor influencing heating energy consumption in office buildings in Harbin[6]. However, existing studies primarily focus on early-stage urban design for new developments, failing to address China's current emphasis on stock optimisation through "retention, renovation, and demolition" (RRD).

Hui et al. analysed the impact of retrofitting strategies on individual building energy consumption in Shanghai's existing residential areas using Grasshopper, ENVI-met, and EnergyPlus, recommending priority measures for hot summer and warm winter zones[7]. Ning et al. proposed microclimate-based design strategies—such as green spaces and activity zones—to enhance thermal comfort in Beijing's traditional courtyards[8]. While these studies address building-level retrofitting, few explore the energy implications of morphological and layout adjustments at the planning scale.

China's urbanisation has transitioned from large-scale demolition to RRD-based stock optimisation. In alignment with human-centric urban development principles, cities are prioritising the renovation of ageing residential areas. Historical districts, as carriers of traditional architectural heritage, require preservation of street patterns and morphology while integrating organic renewal strategies. Under the "dual carbon" goals, energy consumption during renovation must also be addressed.

Since Nanjing's designation as a National Historical and Cultural City in 1982, the municipality has accumulated extensive experience in preserving traditional residential areas. This study selects a plot in Nanjing's Lotus Pond Historical District for parametric modelling, exploring RRD-based renewal strategies to reduce energy use intensity (EUI) and analysing correlations between morphological parameters and energy consumption. The findings offer guidance for low-energy retrofitting of historical residential districts.

1. Study Scope

The Lotus Pond Historical District, located in Nanjing's southern Shuangtang Subdistrict, represents a Ming-Qing dynasty residential and silk-weaving neighbourhood. The Lotus Pond Conservation Plan mandates protection of historical streets, courtyards, and architectural heritage while permitting adaptive reuse to enhance sustainability.

The study focuses on a 6,231.35 m² northwestern plot (Figure 1), bordered by Yingao Lane (north), Mingyangli (south), Mingyang Street (west), and Xiaoshunli (east). Of the 33 buildings within the plot, 28 are traditional or general structures targeted for renovation (Figure 2). Parametric models in Rhino simplified buildings to flat-roofed forms with uniform 4-metre floor heights.

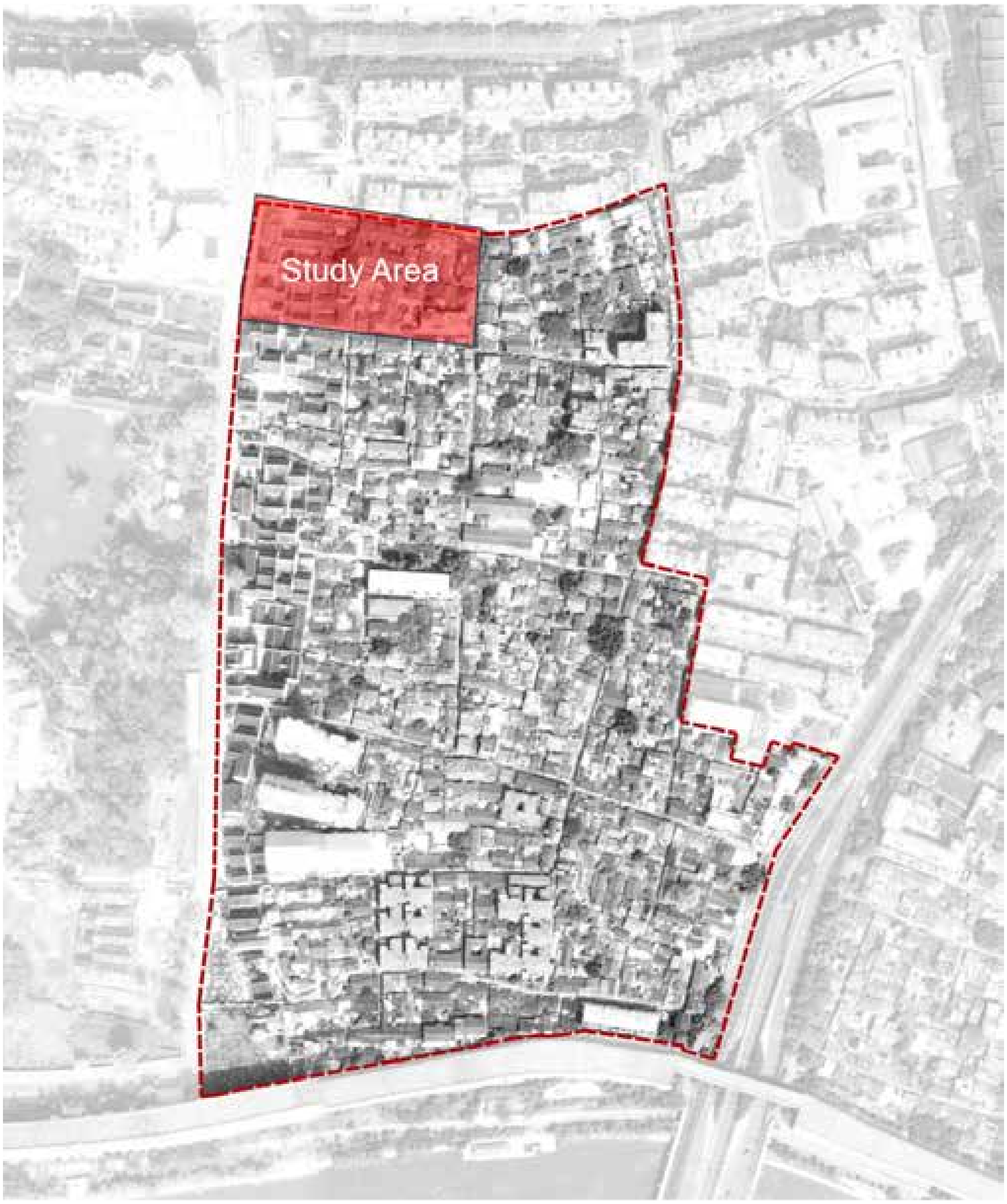

Figure 1 Study Area Boundary

Figure 2 Site Modeling and Renovation Scope Map

2. Simulation of Renovation Schemes

2.1 Height Adjustment Optimisation for Low EUI

The simulation and optimisation processes were conducted entirely within the Grasshopper platform in Rhino. Using the HB Model to OSM component in Grasshopper, Honeybee models were converted to OpenStudio models. Inputting Nanjing's meteorological parameters enabled the calculation of annual total energy consumption, including heating, cooling, indoor lighting, and equipment usage. Heating and cooling temperature thresholds in Honeybee were based on the ASHRAE 55 adaptive thermal comfort model, triggering heating below 18°C (64.4°F) and cooling above 28°C (82.4°F).

The building morphology generation logic retained the original building footprints, with randomised seed numbers controlling floor count variations (1–4 stories). The Annealing Solver in the Genome component (a simulated annealing algorithm) optimised schemes for low EUI. Simulated annealing, inspired by physical annealing processes, is suited for single or few-parameter optimisation. During the initial high-temperature phase, the algorithm explores a broad search space to avoid local optima. In the low-temperature phase, it refines solutions within a narrower range, converging toward the global optimum. Parameter settings for the simulated annealing algorithm are detailed in Table 1.

Table 1. Simulated Annealing Algorithm Parameters

Simulation parameters	Numerical value
Meteorological parameters of Nanjing City	chn_jiangsu.nanjing.582380_cswd
Building type	Midrise Apartment
Simulation cycle	From 00:00 on January 1st to 24:00 on December 31st
Floor height	4 meters
The range of changes in the number of layers	1-4 floors /1-2 floors
Gene	Random number of seeds (1-100)
Objective	Low EUI
Initial temperature	100%
Cooling rate	0.8
Drift rate	50%

2.2 Solar Radiation Potential Assessment of Renovation Schemes

To investigate the specific causes of EUI reduction during optimisation, solar radiation across all schemes was evaluated. Morphological changes, such as building height adjustments, may alter self-shading effects, reducing solar heat gain and thus cooling demand. Additionally, height modifications influence the shape coefficient (*S/V*), defined as the ratio of building surface area to volume, which affects thermal loss or gain. Therefore, solar radiation analysis is critical for each scheme.

For intuitive comparison of solar potential, the Zhejiang Provincial Construction Standard DB33/1105-2014 Code for Renewable Energy Application Accounting in Civil Buildings (Article 4.1.2) stipulates: "Roof areas with annual solar radiation exceeding 625 kW·h/(m²·a) should be prioritised for solar collector or photovoltaic panel installation." Given Nanjing's proximity to Zhejiang, this threshold was adopted.

Meteorological data, simulation periods, sensor locations, grid resolution (2m), and surface reflectivity parameters were configured as detailed in Table 2. The models and parameters were input into the Grasshopper workflow to simulate solar radiation, with results statistically analysed.

Solar radiation simulations were conducted using the Ladybug and Honeybee plugins integrated into Rhino's Grasshopper platform, leveraging the Radiance calculation engine. This method holistically accounts for building dimensions, orientation, ground reflectance, and adjacent structure reflections, generating accurate radiation values for roofs and façades across the case study (Figure 3).

Table 2. Settings of Solar Radiation Simulation Parameters

Simulation parameters	Numerical value
Meteorological data	https://climate.onebuilding.org/WMO_Region_2_Asia/CHN_China/JS_Jiangsu/CHN_JS_Nanjing.582380_TMYx.zip
Simulation cycle	From 00:00 on January 1st to 24:00 on December 31st
Measurement point position	100mm above the grid
Grid size	2 mx2 m
Building surface reflectivity	0.2
Average ground reflectivity	0.2

In this study, solar radiation potential was determined by calculating the ratio of the area exceeding the solar radiation threshold to the total exterior surface area of buildings across different simulated schemes. Using Grasshopper's component settings, measurement points surpassing the threshold were visually highlighted in the model (Figure 3). The proportion of highlighted points relative to the total measurement points served as a comparative metric for evaluating solar energy utilisation potential.

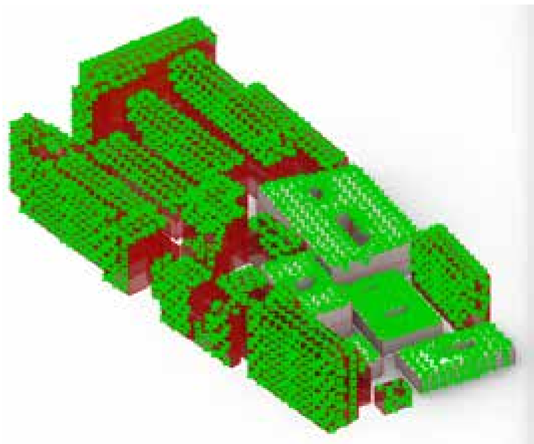

Figure 3 High-Radiation Zones (Threshold: 625 kWh/m²/a)

2.3 Correlation Analysis
Building morphological parameters and simulation results for all schemes were recorded and imported into SPSS software. Pearson correlation analysis was conducted between indicators to investigate the causes and logic behind EUI reduction in optimised schemes. The Pearson correlation coefficient (*r*) ranges from -1 (indicating a perfect negative linear correlation) to 1 (perfect positive linear correlation), with 0 signifying no linear correlation. A significance level of rat 0.01 (two-tailed) indicates statistically significant correlations.

3. Research Conclusions
3.1 Optimisation Results
The baseline EUI of the original scheme was 303.354 kWh/m². Simulation results identified 22 optimal schemes (Table 3), with unchanged energy consumption for indoor lighting (8.866 kWh/m²) and equipment (32.119 kWh/m²). The EUI of optimal schemes decreased by approximately 25 kWh/m² compared to the baseline.

Under heritage conservation guidelines—"strict protection of existing heights for heritage conservation units and historical buildings; new buildings restricted to ≤2 stories with eave heights ≤7 metres"—a secondary simulation constrained building heights to 1–2 stories. This achieved a further EUI reduction of 5.6 kWh/m².

Solar radiation potential (Table 4) decreased across low-EUI optimised schemes. The baseline potential (31.23%) was reduced post-height adjustment. Schemes 14, 16, and 22 exhibited relatively higher potential (>28%), while Schemes 2, 4, 5, 9, and 12 showed lower potential (<22%). This decline likely stems from increased self-shading effects resulting from taller building heights in optimised schemes.

3.2 Correlation Analysis
A Pearson correlation analysis between EUI results from two height adjustment phases and the shape coefficient (*S/V*) revealed a strong positive correlation (Figure 4). Further analysis of energy consumption data, morphological parameters, and annual solar radiation simulations (via SPSS) yielded the following key results (Table 5):

1 Floor area ratio (FAR) exhibited significant negative correlations with solar radiation potential, EUI, and heating/cooling energy demands.

2 Shape coefficient (*S/V*) showed significant positive correlations with solar radiation potential, EUI, and heating/cooling energy demands.

3∆Solar radiation potential correlated positively with EUI, cooling energy consumption, and *S/V*.

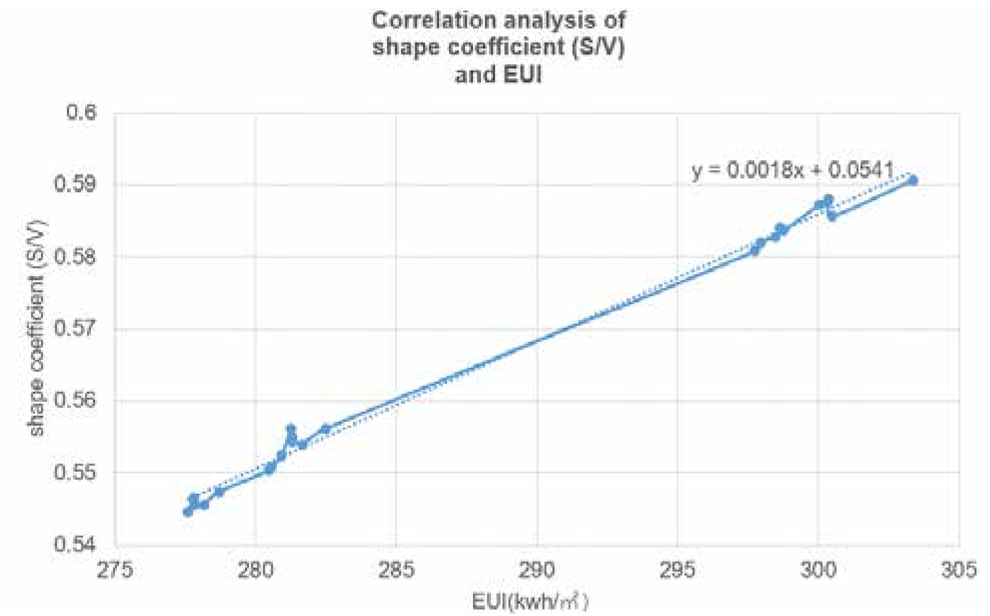

Figure 4 Correlation analysis of shape coefficients and EUI

3.3 Optimisation Recommendations

Floor area ratio (FAR) and shape coefficient (S/V) are critical morphological parameters influencing energy consumption. Reducing FAR (<1.2) and S/V (≤0.55) significantly decreases heating and cooling demands.

Adjusting building heights reduced EUI by 8.3% (approximately 25 kWh/m²). However, solar radiation potential decreased by 9.4% due to increased shading. Designs must balance energy efficiency with solar utilisation.

High solar radiation zones (>28%) should prioritise photovoltaic installations, but shading effects caused by taller buildings must be mitigated.

Adopt the "retain, renovate, demolish, and rebuild" (RRD) approach to preserve traditional urban fabric while optimising morphological parameters. Integrate parametric tools for precise energy consumption prediction and scheme optimisation, supporting green renewal of historical districts under China's "dual carbon" goals (carbon peaking and neutrality).

Appendix

Table 3. Simulation of Height Transformation

Scheme Serial number	Picture	Energy consumption parameter (kwh/)			Architectural form parameters			
		EUI	Heating	Cooling	Total building area	Total building volume m³	Floor area ratio (FAR)	shape coefficient (S/V)
Original plan	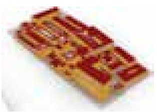	303.354	185.344	77.026	4470.19	19837.16	0.796	0.5906
1	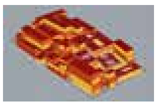	277.611	163.635	72.991	7365.40	31418.07	1.260	0.5446
2	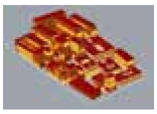	277.791	163.858	72.948	7525.55	32058.67	1.286	0.5465
3	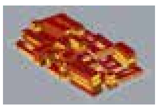	277.837	163.842	73.011	7406.34	31581.81	1.267	0.5456
4	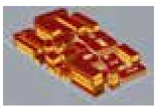	278.155	164.162	73.008	7259.97	30996.00	1.244	0.5456
5	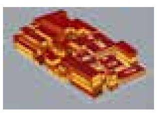	278.716	164.616	73.116	7350.68	31359.18	1.258	0.5474
6	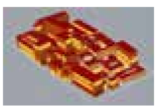	280.476	166.010	73.481	6943.00	29728.47	1.190	0.5503

7	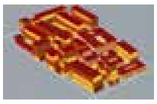	280.567	166.006	73.577	6926.09	29660.83	1.190	0.5508
8	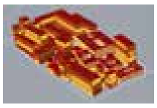	280.942	166.093	73.865	7077.33	30265.80	1.210	0.5525
9	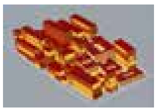	281.275	166.377	73.912	7632.48	32486.41	1.300	0.5561
10	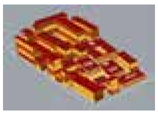	281.280	166.609	73.686	7265.65	31019.07	1.240	0.5544
11	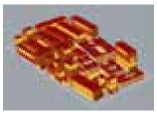	281.310	166.561	73.765	7367.87	31427.95	1.261	0.5551
12		281.663	167.128	73.550	7018.57	30030.76	1.205	0.5539
13		282.481	167.748	73.748	7036.8	30103.68	1.208	0.5561
14		297.754	180.872	75.897	4870.18	21437.19	0.860	0.5808
15		297.939	180.879	76.075	4937.07	21704.75	0.870	0.5820
16		298.492	181.397	76.111	4899.04	21552.63	0.865	0.5828
17	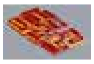	298.640	181.682	75.973	4982.56	21886.72	0.880	0.5841
18		298.781	181.774	76.023	4894.11	21532.91	0.860	0.5837
19		300.029	182.633	76.411	4934.84	21695.83	0.870	0.5872
20		300.348	182.924	76.440	4881.86	21483.91	0.862	0.5876

21	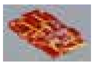	300.364	182.849	76.531	4884.05	21492.68	0.862	0.5881
22	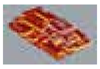	300.501	183.118	76.398	4694.96	20736.32	0.832	0.5857

Table 4. Simulation Results of Solar Radiation

Scheme Serial number	Picture	Solar radiation potential (%)	Scheme Serial number	Picture	Solar radiation potential (%)
Original plan	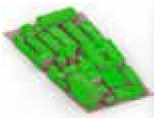	31.23			
1	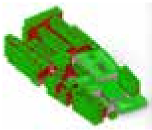	22.27	12	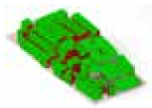	21.82
2	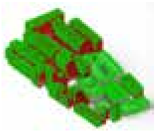	21.64	13	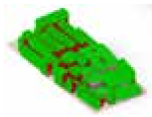	22.65
3	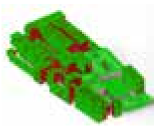	22.36	14	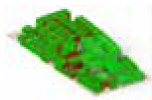	28.01
4	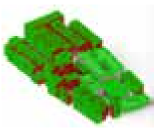	21.96	15	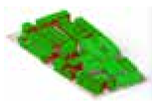	27.90
5	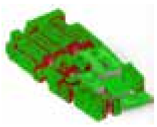	21.78	16	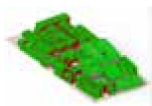	28.02
6	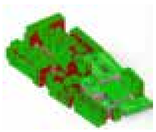	22.93	17	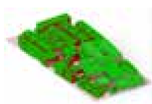	26.59
7	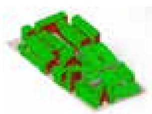	22.90	18		27.54
8	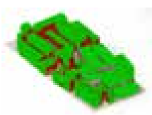	22.89	19	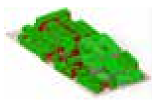	27.56

Scheme Serial number	Picture	Solar radiation potential (%)	Scheme Serial number	Picture	Solar radiation potential (%)
9	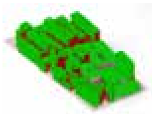	21.73	20	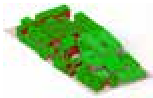	27.90
10	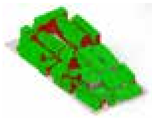	22.37	21		27.85
11	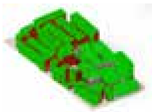	21.69	22	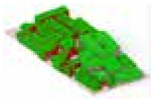	28.86

Table 5. Correlation Analysis

	Solar radiation potential (%)	EUI (kwh/)	Heating energy consumption (kwh/)	Cooling energy consumption (kwh/)	Floor area ratio (FAR)	shape coefficient (S/V)
Solar radiation potential (%)	--					
EUI (kwh/)	.972**					
Heating energy consumption (kwh/)	.972**	1.000**	--			
Cooling energy consumption (kwh/)	.969**	.996**	.994**	--		
Floor area ratio (FAR)	-.980**	-.989**	-.990**	-.977**	--	
shape coefficient (S/V)	.957**	.997**	.996**	.996**	-.976**	--

References

[1] China Building Energy Conservation Association, China building energy consumption research report, Architecture 2 (2019) 26–31.

[2] A. Salvati, H. Coch, Urban climate and building energy performance in compact cities in Mediterranean climate, in: M. Palme, A. Salvati (Eds.), Urban Microclim. Model. Comf, Energy Stud., Springer International Publishing, Cham, 2021, pp. 105–135, https://doi.org/10.1007/978-3-030-65421-4_6.

[3]Mengju X ,Minghao W ,Hua Z , et al.The impact of urban morphology on the building energy consumption and solar energy generation potential of university dormitory blocks[J].Sustainable Cities and Society,2023,96

[4]Shen X ,Mengcheng S ,Mengju X , et al.Influence of urban morphological factors on building energy consumption combined with photovoltaic potential: A case study of residential blocks in central China[J].Building Simulation,2023,16(9):1777-1792.

[5] Y. Li, D. Wang, S. Li, W. Gao, Impact analysis of urban morphology on residential district heat energy demand and microclimate based on field measurement data, Sustainability. 13 (2021) 2070, https://doi.org/10.3390/su13042070.

[6] H. Leng, X. Chen, Y. Ma, N.H. Wong, T. Ming, Urban morphology and building heating energy consumption: Evidence from Harbin, a severe cold region city, Energy Build. 224 (2020) 110143, https://doi.org/10.1016/j.enbuild.2020.110143.

[7]Hui Y ,Huibo Z ,Luo Q , et al.Evaluation of renovation strategies for existing residential districts in Shanghai based on coupling calculation of microclimate and energy consumption[J].Energy & Buildings,2023,298

[8]Ning L ,Zhao G ,Wenying G , et al.Design strategies for renovation of public space in Beijing's traditional communities based on measured microclimate and thermal comfort[J].Sustainable Cities and Society,2023,99